

Supporting Information

A Pure Red Luminescent β -Carboline-Substituted Biphenylmethyl Radical: Photophysics, Stability and OLEDs

*Alim Abdurahman, Yingxin Chen, Xin Ai, Ablikim Obolda, Yu Gao, Shengzhi Dong,
Bao Li, Bing Yang, Ming Zhang and Feng Li**

Contents

S1. Experimental section.....

S2. MALDI-TOF mas spectra and FT-IR spectra of PyID-BTM.....

Fig. S1 and S2

S3. Crystallographic data of PyID-BTM.....

Table S1

S4. Selected angles in the crystal of PyID-BTM.....

Table S2

S5. Therma and Electrochemical properties.....

Fig. S3, S4 and S5.

S6. Spin density distribution calculated using DFT

Fig. S6.

S7. Measurements and calculations of molar extinction coefficients (ϵ).....

Fig. S7 and S8

S8. Solvation Effect of PyID-BTM.....

Table S3

S9. Current efficiency (CE) and Power efficiency (PE) versus current density curves..

Fig. S9

S10. EL spectra of PyID-BTM-based OLEDs with different doping concentration at different voltages.....

Fig. S10

S11. EPR spectra of PyID-BTM before and after evaporation.....

Fig. S11

S11. Data of DFT and TD-DFT calculations.....

S1. Experimental Section

General: All reagents and solvents were purchased from commercial sources and used as received unless otherwise stated. Chromatographic separations were carried out using silica gel (200-300 mesh). The ¹H nuclear magnetic resonance (NMR) spectra were obtained in deuterated dimethyl sulfoxide (DMSO) with a Bruker Avance-III 500 NMR spectrometer at ambient temperature. Fourier transform infrared spectroscopy (FTIR) spectra of radicals were recorded with Brucker VERTEX 80V. MALDI-TOF mass spectra were recorded on a Brucker Autoflex speed TOF/TOF mass spectrometer with DCTB as a matrix. EPR spectra were recorded on a Bruker ELEXSYS-II E500 CW-EPR spectrometer at ambient temperature. Thermal gravimetric analysis (TGA) was carried out on the Pyris1 TGA thermal analysis system at a heating rate of 20 °C min⁻¹ in a nitrogen atmosphere. Ultraviolet-visible (UV-Vis) absorption spectra were recorded on a shimadzu UV-2550 spectrophotometer. Fluorescence spectra were performed using a RF-5301 PC spectrophotometer. The CV measurements were performed using an electrochemical analyzer (CHI660C, CH Instruments, USA). A glass carbon disk was used as the working electrode. A platinum wire acted as the counter electrode and Ag/Ag⁺ acted as the reference electrode together with the redox couple ferrocenium/ferrocene as the internal standard at the rate of 50 or 100 mV·s⁻¹. Tetrabutylammonium hexafluorophosphate (TBAPF₆) in anhydrous dichloromethane (0.1 M) were used as the supporting electrolyte for negative and positive scan respectively. (The measured electrochemical data of CzBTM was slightly different form that reported previously. This may be duo to the fact that the electrode used is

different from those used before). An Edinburgh fluorescence spectrometer (FLS980) was used for the fluorescence decay and absolute fluorescence measurements. The lifetime of the excited states was measured by the time-correlated single photon counting method (detected at the peak of the PL) under the excitation of a laser (375 nm) with a pulse width of 50 ps.

Magnetic measurements were performed on a Quantum Design 6.5 Tesla SQUID-VSM system with a temperature range of 2-300 K and an applied field of 1000 Oe. After correction of diamagnetic contributions from the sample, using tabulated constants, sample holder, and paramagnetic contamination, the magnetic data were fitted with Curie-Weiss law. “ $\chi_m = C/(T-\theta)$ ” where C is Curie constant and θ is Weiss temperature.

Photostability of radicals was tested under irradiation with a 355 nm pulse laser (power density: 195.4 kW/cm², pulse width: 8 ns, frequency: 10 Hz).

The single crystals suitable for X-ray structural analysis were obtained by slow evaporation from the chloroform/ethanol solution at room temperature. Single crystal X-ray diffraction data were collected on a Rigaku RAXIS-PRID diffractometer using the ω -scan mode with graphite-monochromator Mo K α radiation ($\lambda = 0.71073 \text{ \AA}$). The structure was solved with direct methods using the SHELXTL programs and refined with full-matrix least squares on F^2 . The corresponding CCDC reference number (CCDC: 1831917) for PyID-BTM. These data can be obtained free of charge from The Cambridge Crystallographic Data Centre via www.ccdc.cam.ac.uk/data_request/cif.

OLED Fabrication and Measurements: The OLEDs were fabricated through vacuum deposition of the materials at $\approx 3\text{--}4 \times 10^{-6}$ mbar onto ITO-coated glass substrates having a sheet resistance of $\approx 30 \Omega^{-2}$. Ready-made indium tin oxide (ITO) glass substrates were purchased and cleaned with ethanol, acetone, toluene and isopropyl alcohol. After dried with N_2 , they were treated with UV irradiation for 15 min. The MoO_3 layer was deposited at a rate of 0.2 \AA s^{-1} . All the organic layers were deposited at $0.4\text{--}0.6 \text{ \AA s}^{-1}$. The evaporation rate of cathode LiF and Al metal layer were 0.1 \AA s^{-1} and $0.6\text{--}1.2 \text{ \AA s}^{-1}$ respectively. The EL spectra, CIE coordinates, and The current density-voltage-luminance (J-V-L) characteristics of the devices were measured with a PHOTO RESEARCH SpectraScan PR 655 photometer and a KEITHLEY 2400 SourceMeter constant current source at room temperature.

Lippert-Mataga calculation: To further understand the effect of solvent polarity on the excited state of PyID-BTM, we used the Lippert-Mataga equation, a model that describes the interactions between the solvent and the dipole moment of solute:

$$\hbar c(v_a - v_f) = \hbar c(v_a^0 - v_f^0) - \frac{2(\mu_e - \mu_g)^2}{a^3} f(\epsilon, n)$$

where f is the orientational polarizability of the solvent, $(v_a^0 - v_f^0)$ corresponds to the Stokes shifts when f is zero, μ_e is the excited state dipole moment, μ_g is the ground-state dipole moment; a is the solvent cavity (Onsager) radius (5.98 \AA), derived from the Avogadro number (N), molecular weight (M), and density ($d=1.0 \text{ g/cm}^3$); ϵ and n are the solvent dielectric and the solvent refractive index, respectively; $f(\epsilon, n)$ and a can be calculated respectively as follows:

$$f(\epsilon - n) = \frac{\epsilon - 1}{2\epsilon + 1} - \frac{n^2 - 1}{2n^2 + 1}, \quad a = \left(\frac{3M}{4N\pi d}\right)^{1/3}$$

The detailed data are listed in Table S1. In low-polarity solvents (slope value ~ 1321, R= 0.52), the corresponding μ_e was estimated to be 5.3 D. In high-polarity solvents (slope value ~ 5295, R= 0.96), the corresponding μ_e was estimated to be 10.6 D.

M1 was prepared according to the literature.¹

¹H NMR (500 MHz, DMSO) δ 10.63 (s, 1H), 7.35 (d, J = 7.7 Hz, 1H), 7.26 (d, J = 8.0 Hz, 1H), 6.99 (t, J = 7.4 Hz, 1H), 6.93 (t, J = 7.3 Hz, 1H), 3.86 (s, 2H), 3.31 (s, 1H), 2.98 (t, J = 5.6 Hz, 2H), 2.59 (t, J = 5.5 Hz, 2H). HRMS (ESI) *m/z*: [M + H]⁺ calcd for C₁₁H₄N₂: 172.1; found: 171.89.

PyID was prepared according to the literature.¹

¹H NMR (500 MHz, DMSO) δ 11.60 (s, 1H), 8.90 (s, 1H), 8.34 (d, J = 5.2 Hz, 1H), 8.24 (d, J = 7.8 Hz, 1H), 8.11 (d, J = 5.2 Hz, 1H), 7.65 – 7.51 (m, 2H), 7.25 (t, J = 7.4 Hz, 1H). HRMS (ESI) *m/z*: [M + H]⁺ calcd for C₁₁H₈N₂: 168.07; found: 167.96

Synthesis of PyID-BTM: Under an argon atmosphere, PyID (0.8 g, 4.76g) in dimethyl sulfoxide (10 ml) solution was added dropwise, with string, a dispersed of sodium hydride (60% in oil, 0.17 g, 7.14 mmol) in anhydrous dimethyl sulfoxide (40 ml). The reaction mixture was stirred for 20 min at room temperature before adding HBTM-Br (1.72 g, 3.82 mmol). And then the mixture was stirred for 4 h under 60 °C. After cooling to room temperature, the mixture was added in saturated ammonium chloride solution (100 ml). The precipitate was collected by suction filtration and

purified by column chromatography (ethyl acetate: petroleum ether = 1:8). Deep red solid PyID-BTM was obtained in 10% (0.21 g) yield. MALDI-TOF(M/S): Calcd for C₂₄H₁₁C_{l6}N₂, 538.90; found, 538.90. Elem.Anal.Calcd for C₂₄H₁₁C_{l6}N₂: C 55.70 , N 2.60 , H 2.24; found: C 55.55 , N 2.51 , H 2.20.

References

- 1 C. Portmann, C. Prestinari, T. Myers, J. Scharte, K. Gademann, *Chembiochem* **2009**, 10, 889.

S2. MALDI-TOF mas spectra and FT-IR spectra of PyID-BTM

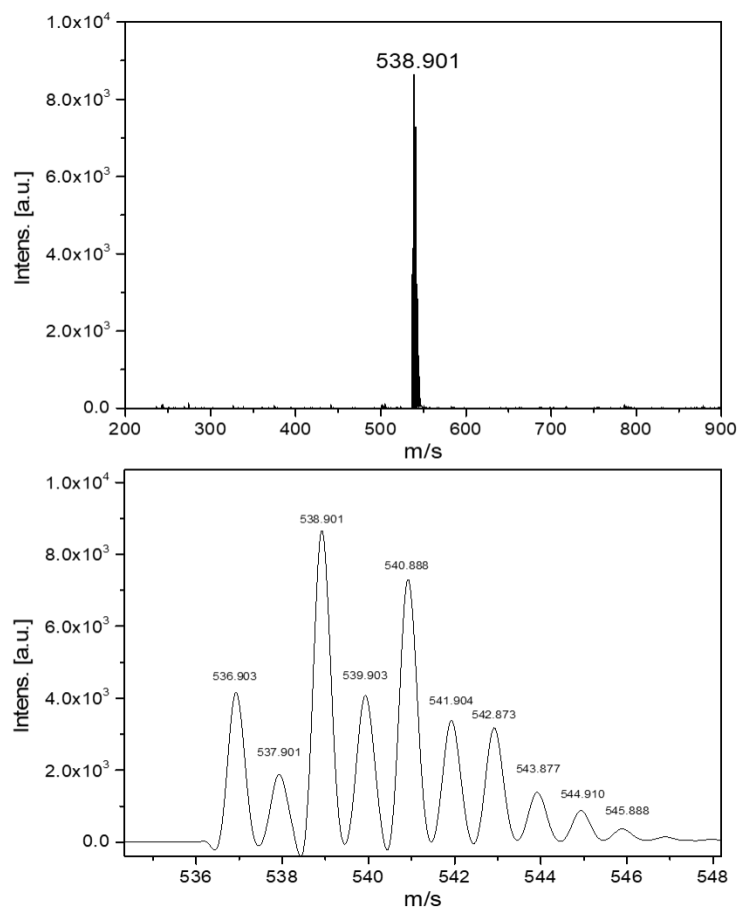


Fig. S1 MALDI-TOF mass spectra of PyID-BTM.

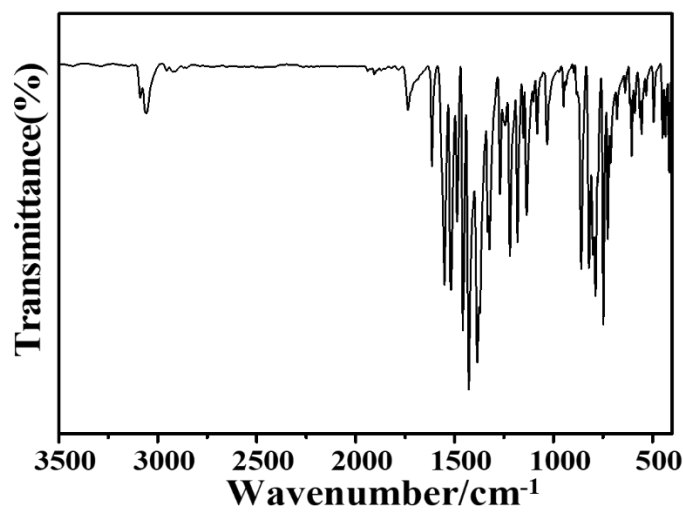


Fig. S2 FT-IR spectra of PyID-BTM.

S3. Crystallographic data of PyID-BTM

Table S1 X-Ray Crystallographic Data of PyID-BTM

CCDC	1831917
Empirical formula	C ₂₄ H ₁₁ Cl ₆ N ₂
Formula weight	540.05
Temperature	273(2) K
Wavelength	0.71073 Å
Crystal system	Monoclinic
Space group	P 21/c
a, Å	16.6879(5)
b, Å	8.2499(2)
c, Å	17.2222(5)
alpha, deg	90
beta, deg	107.7570(10)
gamma, deg	90
Volume, Å ³	2258.08(11)
Z	4
Calculated density, Mg/m ³	1.589
Absorption coefficient, mm ⁻¹	0.778
F(000)	1084
Crystal size, mm ³	0.0500x0.0300x0.0200
Theta range for data collection, deg	2.76 to 28.29
Limiting indices	-22<=h<=21,-10<=k<=10, -22<=l<=21
Reflections collected	25386
Independent reflections	5592 [R(int) = 0.0449]
Completeness to theta = 28.29°	99.7 %
Absorption correction	Semi-empirical from equivalents
Max. and min. transmission	0.985 and 0.972
Refinement method	Full-matrix least-squares on F ²
Data / restraints / parameters	5592 / 0 / 289
Goodness-of-fit on F ²	1.043
Final R indices [I>2sigma(I)]	R1 = 0.0516, wR2 = 0.1296
R indices (all data)	R1 = 0.1048, wR2 = 0.1669
Largest diff. peak and hole, e.Å ⁻³	0.493 and -0.473

S4. Selected angles in the crystal of PyID-BTM

Table S2 Selected angles in the crystal of PyID-BTM.

Angles	$\Phi(\text{PyID-BTM})$
N1C7C8	118.14°
N1C7C6	118.7°
C6C7C8	123.15°
Dihedral angle between N1C6C8 plain (β -carboline moieties)	42.6°
(2,4,6-trichlorophenyl including C7)	49.5°
(2,4,6-trichlorophenyl including C6)	49.6°

S5. Therma and Electrochemical properties

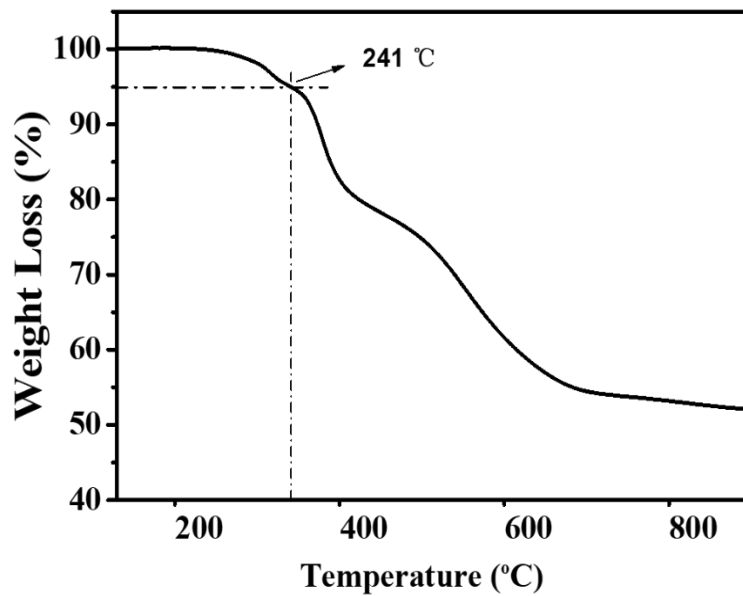


Fig. S3 TGA curve of PyID-BTM under nitrogen flow.

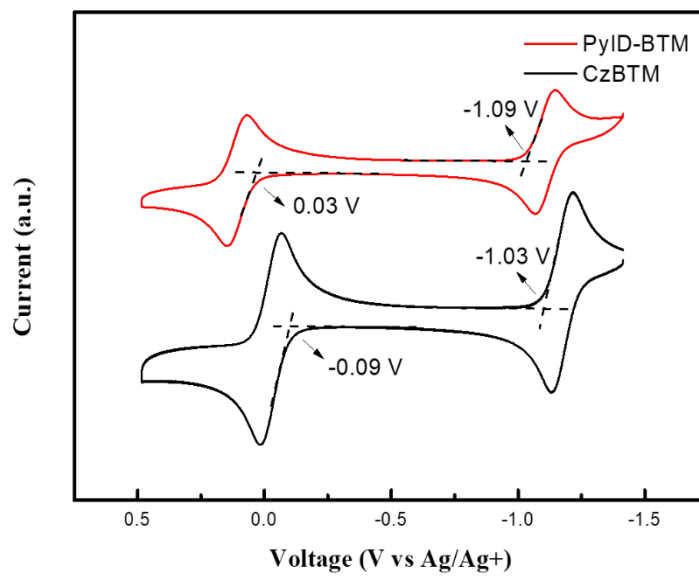


Fig. S4 Cyclic voltammograms of PyID-BTM and CzBTM in 0.1 M TBAPF₆-CH₂Cl₂ at a scan rate of 0.05 Vs⁻¹.

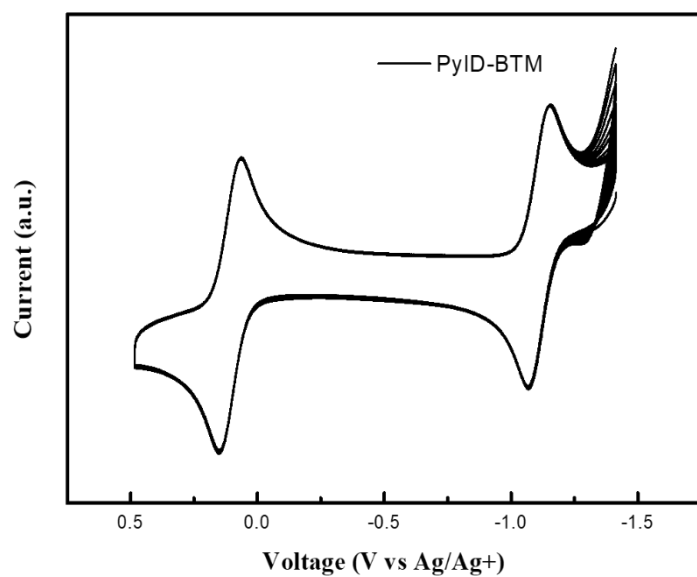


Fig. S5 Multi-cycle CV measurements (20 cycles) of PyID-BTM in 0.1 M TBAPF₆-CH₂Cl₂ at a scan rate of 0.1 Vs⁻¹.

S6. Spin density distribution calculated using DFT.

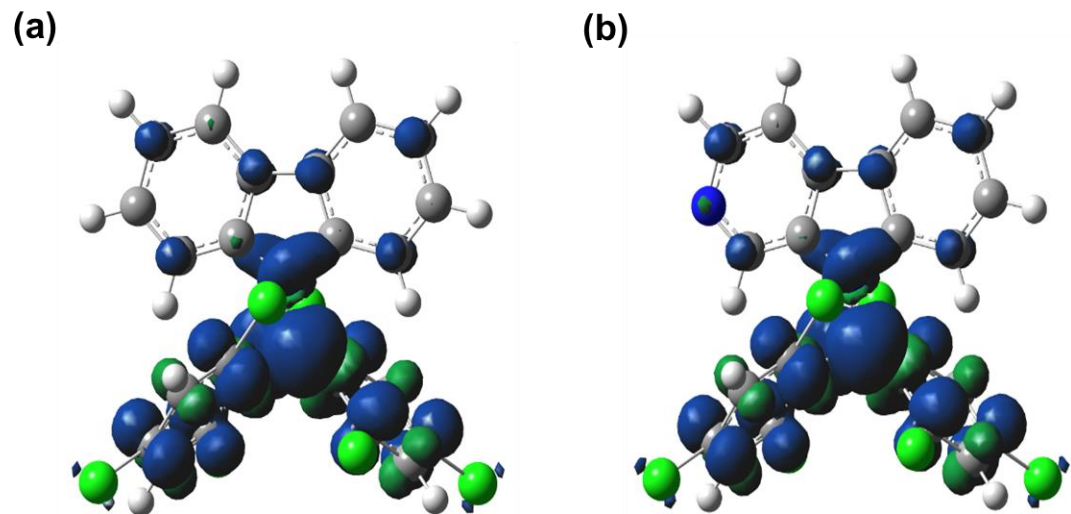


Fig. S6 Spin density distribution of (a) CzBTM and (b) PyID-BTM using DFT methods
(UB3LYP/6-31G(d,p)) with isovalue at 0.0015.

S7. Measurements and calculations of molar extinction coefficients (ϵ)

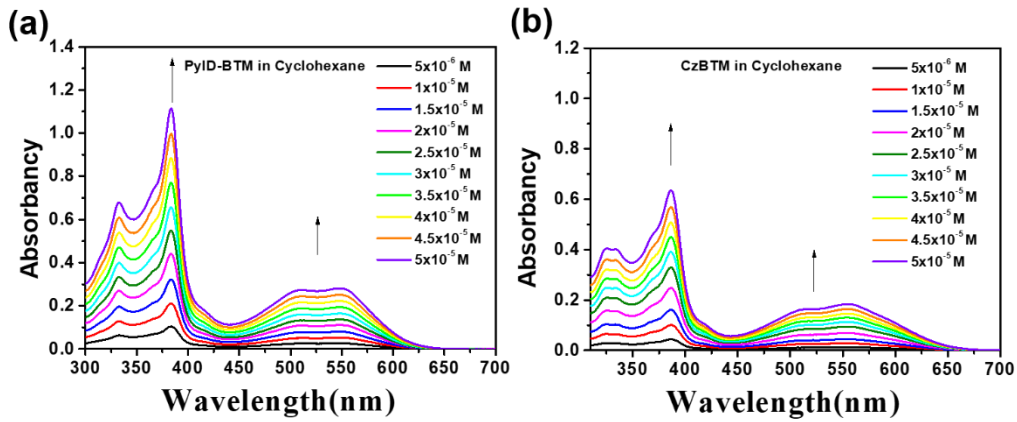


Fig. S7 UV-spectrum of (a) PyID-BTM and (c) CzBTM in cyclohexane at different concentration.

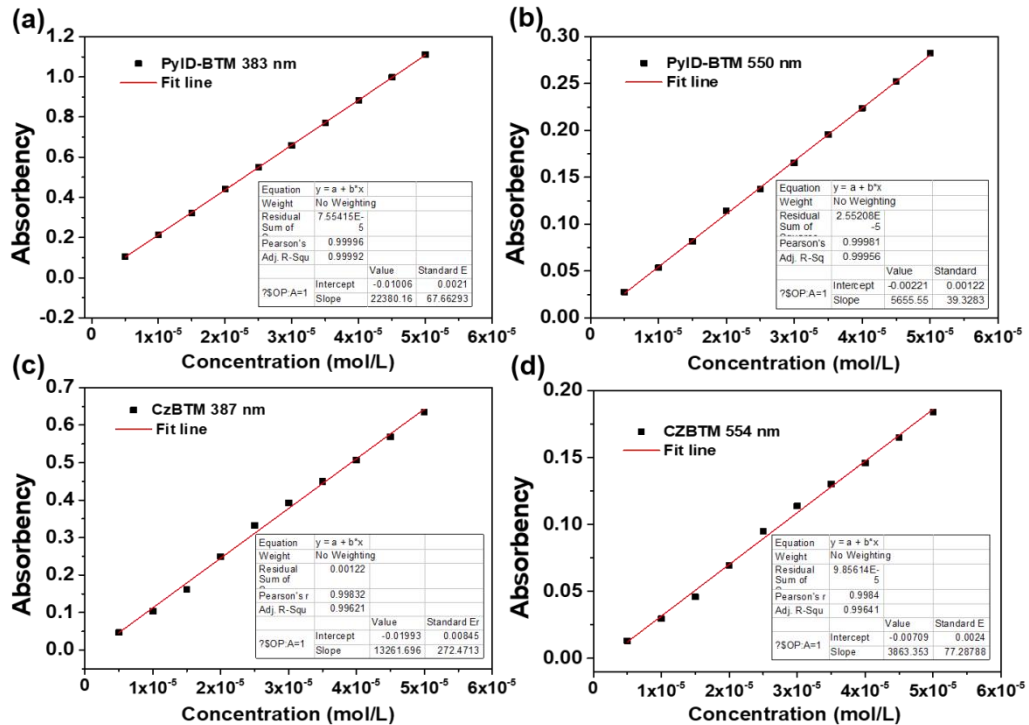


Fig. S8 Absorbency-concentration fitting line of PyID-BTM and CzBTM.

S8. Solvation Effect of PyID-BTM

Table S3 Photophysical properties of PyID-BTM in different solvents.

Solvent	Δf	v_a (nm)	v_b (nm)	v_a-v_b (cm ⁻¹)	FWHM (nm)	Φ_F (%)
Cyclohexane	0	548	664	3188	81	19.51
p-xylene	0.003	547	681	3597	99	4.23
Toluene	0.014	546	682	3652	101	4.05
butyl ether	0.096	544	678	3633	101	3.63
isopropyl ether	0.145	547	684	3661	102	3.82
chloroform	0.149	543	677	3645	99	4.26
diethyl ether	0.167	546	689	3801	107	2.86
Tetrahydrofuran	0.210	545	703	3973	123	0.62
dichloromethane	0.218	544	694	3973	112	2.60
Dimethyl formamide	0.276	544	711	4494	160	0.23
Acetonitrile	0.305	541	711	4420	139	0.3

S9. Current efficiency (CE) and Power efficiency (PE) versus current density curves.

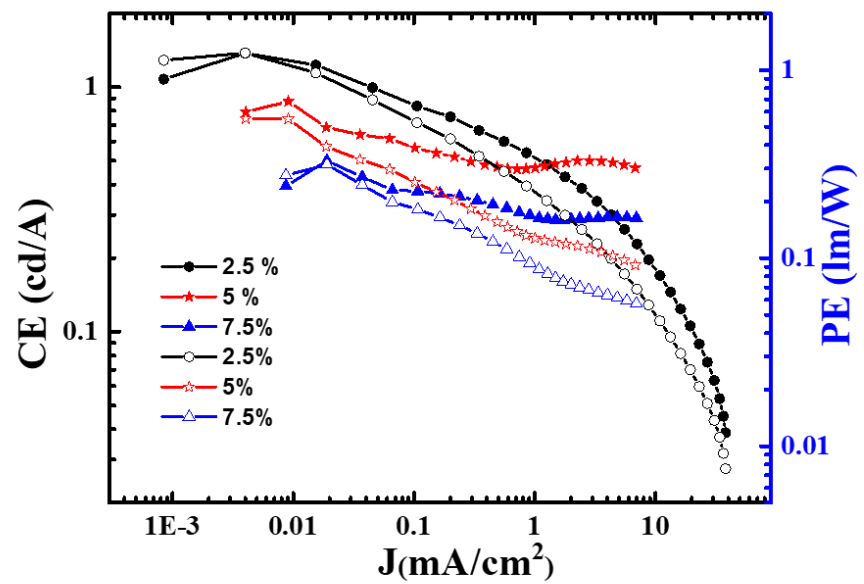


Fig. S9 Current efficiency (CE) and Power efficiency (PE) versus current density curves.

S10. EL spectra of PyID-BTM-based OLEDs with different doping concentration at different voltages

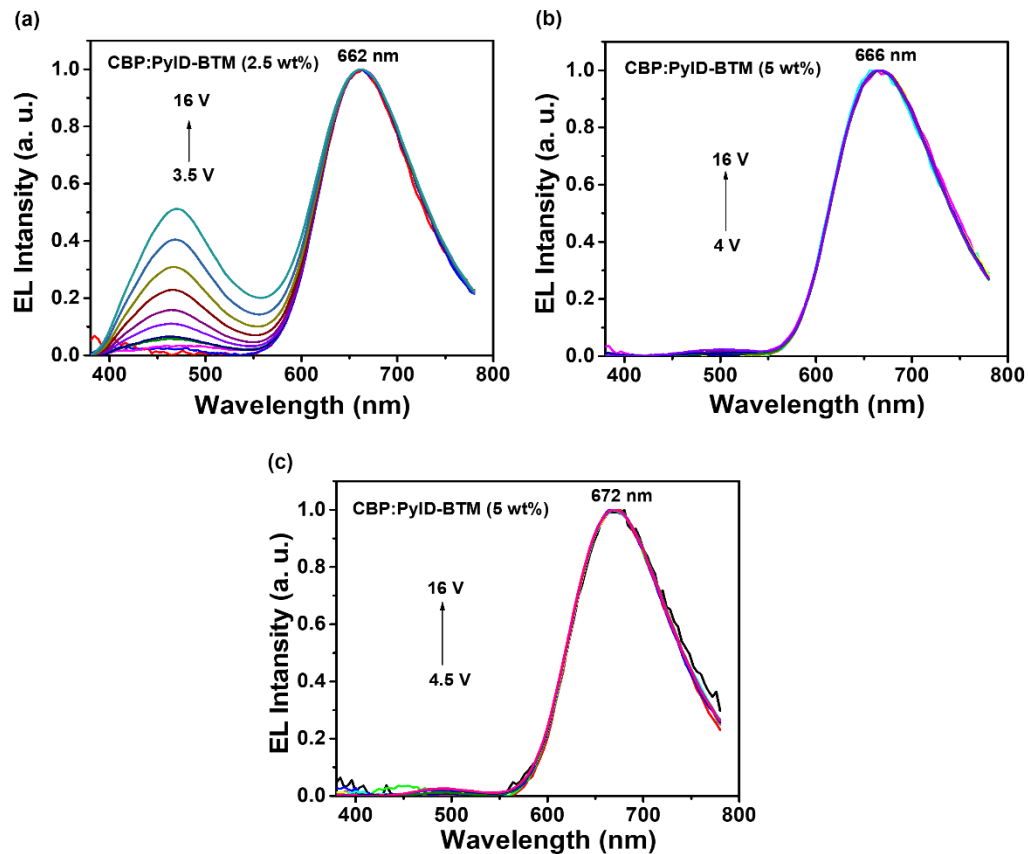


Fig. S10 EL spectra of PyID-BTM-based OLEDs with different doping concentration at Different voltages

S11. EPR spectra of PyID-BTM before and after evaporation

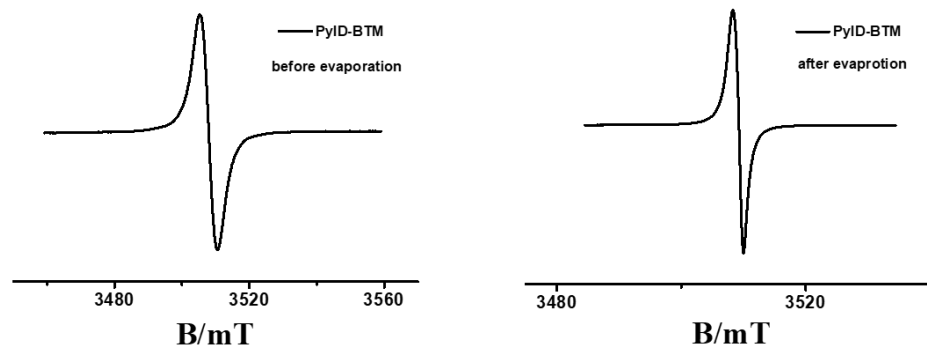


Fig. S11 EPR spectra of PyID-BTM powder measured at room temperature before and after evaporation.

S12. Data of DFT and TD-DFT calculations

Cartesian coordinates of all the optimized geometries by DFT calculation

PYID-BTM (UB3LYP/6-31G(d))

Center Number	Atomic Number	Atomic Type	Coordinates (Angstroms)		
			X	Y	Z
1	6	0	0.002721	-0.072398	0.003823
2	6	0	-1.284546	-0.770775	0.093913
3	6	0	-1.644863	-1.830292	-0.778867
4	6	0	-2.271095	-0.430025	1.058671
5	6	0	-2.866231	-2.492748	-0.709559
6	6	0	-3.504774	-1.065331	1.139201
7	6	0	-3.792494	-2.097000	0.249920
8	1	0	-3.095068	-3.286594	-1.408653
9	1	0	-4.217303	-0.774423	1.900243
10	6	0	1.289059	-0.771506	-0.085584
11	6	0	2.274830	-0.436733	-1.053734
12	6	0	1.648739	-1.829439	0.789634
13	6	0	3.506405	-1.076467	-1.134671
14	6	0	2.867806	-2.496230	0.719783
15	6	0	3.793190	-2.106236	-0.242934
16	1	0	4.217415	-0.791037	-1.899262
17	1	0	3.094930	-3.289797	1.419805
18	17	0	1.950800	0.761656	-2.290053
19	17	0	0.580703	-2.320804	2.093597
20	17	0	-0.574585	-2.330455	-2.077100
21	17	0	-1.945114	0.772164	2.291715
22	17	0	5.337419	-2.923138	-0.335825
23	17	0	-5.338367	-2.909604	0.342930
24	6	0	-0.880410	2.148956	-0.733063
25	6	0	0.873394	2.166022	0.718709
26	6	0	-1.888745	1.828725	-1.645944
27	6	0	-0.568134	3.501577	-0.477698
28	6	0	1.880945	1.835360	1.628190
29	6	0	0.547747	3.515333	0.445310
30	1	0	-2.132357	0.801916	-1.898596
31	6	0	-1.313006	4.488696	-1.124276
32	6	0	2.578708	2.880061	2.230697
33	1	0	2.115741	0.807240	1.870588
34	6	0	1.259226	4.547810	1.063290
35	6	0	-2.317037	4.068926	-1.993259
36	1	0	-1.118734	5.545106	-0.968495

37	6	0	2.280534	4.223281	1.950515
38	1	0	3.368169	2.644756	2.937948
39	1	0	1.011812	5.584944	0.857914
40	1	0	-2.926934	4.801991	-2.516303
41	1	0	2.845039	5.011576	2.438236
42	7	0	0.000489	1.322483	-0.003647
43	7	0	-2.597505	2.780374	-2.258542

CzBTM (UB3LYP/6-31G(d))

Center Number	Atomic Number	Atomic Type	Coordinates (Angstroms)		
			X	Y	Z
1	6	0	0.000037	-0.069737	-0.000077
2	6	0	-1.285358	-0.771511	0.092015
3	6	0	-1.645172	-1.832971	-0.778698
4	6	0	-2.271100	-0.434724	1.059481
5	6	0	-2.863322	-2.501245	-0.705615
6	6	0	-3.502058	-1.075350	1.143683
7	6	0	-3.788359	-2.108751	0.256201
8	1	0	-3.090051	-3.297370	-1.402842
9	1	0	-4.212993	-0.787319	1.907353
10	6	0	1.285383	-0.771541	-0.092128
11	6	0	2.271350	-0.434618	-1.059335
12	6	0	1.644973	-1.833204	0.778434
13	6	0	3.502284	-1.075305	-1.143412
14	6	0	2.863081	-2.501555	0.705446
15	6	0	3.788346	-2.108915	-0.256094
16	1	0	4.213386	-0.787161	-1.906885
17	1	0	3.089600	-3.297860	1.402537
18	17	0	1.948431	0.769220	-2.290591
19	17	0	0.577980	-2.328602	2.082441
20	17	0	-0.578533	-2.328118	-2.083084
21	17	0	-1.947832	0.768854	2.290893
22	17	0	5.332047	-2.927679	-0.353179
23	17	0	-5.332100	-2.927434	0.353424
24	6	0	-0.877819	2.157269	-0.730591
25	6	0	0.877864	2.157261	0.730528
26	6	0	-1.879070	1.814812	-1.641133
27	6	0	-0.557262	3.508073	-0.463820
28	6	0	1.879223	1.814748	1.640930
29	6	0	0.557164	3.508044	0.464013
30	1	0	-2.106937	0.783680	-1.877769

31	6	0	-1.272587	4.531034	-1.091719
32	6	0	2.582322	2.851032	2.254031
33	1	0	2.107210	0.783606	1.877330
34	6	0	1.272396	4.530965	1.092058
35	6	0	-2.290593	4.195895	-1.980775
36	1	0	-1.031601	5.571291	-0.893933
37	6	0	2.290497	4.195835	1.980999
38	1	0	3.368439	2.606447	2.961842
39	1	0	1.031253	5.571222	0.894432
40	1	0	-2.856704	4.979454	-2.474703
41	1	0	2.856546	4.979347	2.475040
42	7	0	0.000065	1.323148	-0.000110
43	6	0	-2.582252	2.851124	-2.254088
44	1	0	-3.368292	2.606555	-2.961990

Excited states calculated by TD-DFT calculations

PyID-BTM (UB3LYP/6-31G(d))

Excited State 1: 2.058-A 2.2587 eV 548.92 nm f=0.1113 <S**2>=0.809
135B ->136B 0.98685

This state for optimization and/or second-order correction.

Total Energy, E(TD-HF/TD-KS) = -3791.76162303

Copying the excited state density for this state as the 1-particle RhoCl density.

Excited State 2: 2.165-A 2.6204 eV 473.16 nm f=0.0199 <S**2>=0.922
135A ->137A 0.10657
136A ->137A 0.59831
129B ->136B -0.11358
132B ->136B -0.22771
134B ->136B 0.70452

Excited State 3: 2.166-A 2.6479 eV 468.23 nm f=0.0335 <S**2>=0.923
135A ->137A -0.10228
136A ->137A -0.64970
129B ->136B 0.20735
132B ->136B 0.12449
134B ->136B 0.66944

Excited State 4: 2.343-A 2.9308 eV 423.04 nm f=0.0068 <S**2>=1.122

135A ->138A	-0.12850
136A ->138A	0.95504
135B ->138B	0.19097

Excited State 5: 2.116-A 3.0474 eV 406.85 nm f=0.0042 <S**2>=0.870

135A ->139A	0.10352
136A ->137A	-0.11154
136A ->139A	0.82243
130B ->136B	-0.34260
131B ->136B	-0.26199
132B ->136B	-0.26246
133B ->136B	0.12017

Excited State 6: 2.165-A 3.1313 eV 395.95 nm f=0.0072 <S**2>=0.922

136A ->139A	0.11944
136A ->140A	0.62765
130B ->136B	-0.41158
131B ->136B	0.50462
132B ->136B	0.23663
133B ->136B	-0.19623

Excited State 7: 2.225-A 3.1547 eV 393.01 nm f=0.0763 <S**2>=0.988

136A ->137A	-0.27264
136A ->139A	-0.17560
136A ->140A	0.12933
136A ->141A	-0.17071
128B ->136B	0.21922
129B ->136B	-0.16111
131B ->136B	0.33786
132B ->136B	-0.39400
133B ->136B	0.61122

Excited State 8: 2.413-A 3.2020 eV 387.20 nm f=0.0500 <S**2>=1.205

129A ->137A	0.13425
130A ->139A	0.10257
132A ->137A	0.12829
134A ->138A	-0.10278
135A ->141A	-0.10892
136A ->137A	0.18207
136A ->140A	-0.21299
136A ->141A	-0.35822
136A ->143A	-0.14821
128B ->136B	0.50542
129B ->136B	0.10790

129B ->137B	-0.11443
130B ->136B	-0.13257
130B ->139B	-0.11859
132B ->136B	0.46928
132B ->137B	-0.10710
133B ->136B	0.15450
134B ->138B	-0.10550

Excited State 9: 2.598-A 3.2707 eV 379.07 nm f=0.0088 <S**2>=1.437

134A ->138A	-0.29760
135A ->144A	0.12636
136A ->139A	-0.20777
136A ->140A	0.19455
136A ->141A	0.15868
136A ->144A	-0.16098
128B ->136B	-0.22752
129B ->136B	-0.16915
130B ->136B	-0.17253
131B ->136B	-0.34082
132B ->136B	0.18902
133B ->136B	0.50508
134B ->136B	0.13489
134B ->138B	-0.30683
135B ->143B	-0.10496

Excited State 10: 2.300-A 3.2824 eV 377.72 nm f=0.0381 <S**2>=1.073

134A ->138A	0.16983
136A ->137A	0.12277
136A ->139A	0.31891
136A ->141A	0.13001
136A ->144A	0.10916
128B ->136B	-0.17982
129B ->136B	0.23640
130B ->136B	0.40262
131B ->136B	0.16409
132B ->136B	0.41698
133B ->136B	0.49601
134B ->138B	0.19457

Excited State 11: 2.500-A 3.2979 eV 375.94 nm f=0.0558 <S**2>=1.313

134A ->138A	-0.27252
135A ->144A	0.10070
136A ->137A	-0.18082
136A ->139A	0.30894

136A ->140A	-0.11985
136A ->144A	-0.13334
129B ->136B	-0.43705
130B ->136B	0.47077
131B ->136B	0.38846
133B ->136B	-0.10380
134B ->138B	-0.26998

Excited State 12: 2.161-A 3.3460 eV 370.55 nm f=0.0057 <S**2>=0.918

136A ->140A	0.65462
136A ->141A	-0.20574
128B ->136B	0.21656
130B ->136B	0.46002
131B ->136B	-0.42629
132B ->136B	-0.10645

Excited State 13: 2.519-A 3.4606 eV 358.28 nm f=0.0361 <S**2>=1.336

134A ->138A	-0.36943
129B ->136B	0.70680
130B ->136B	0.14529
131B ->136B	0.19234
132B ->136B	-0.37918
134B ->138B	-0.28056

Excited State 14: 2.603-A 3.6864 eV 336.33 nm f=0.1073 <S**2>=1.444

135A ->138A	0.22476
136A ->138A	0.11849
136A ->140A	0.11183
136A ->141A	0.69635
136A ->145A	-0.14869
128B ->136B	0.35446
135B ->138B	-0.33681

Excited State 15: 3.264-A 3.7781 eV 328.17 nm f=0.0120 <S**2>=2.414

128A ->137A	-0.12128
130A ->139A	-0.25237
130A ->140A	-0.16486
131A ->139A	0.23068
131A ->140A	-0.24896
132A ->140A	-0.11717
135A ->137A	0.35202
136A ->137A	-0.15214
136A ->142A	0.13720
128B ->137B	0.16181

129B ->136B	0.28641
130B ->139B	0.23213
130B ->140B	0.17211
131B ->139B	-0.22856
131B ->140B	0.23438
132B ->136B	0.19305
132B ->140B	0.10796
135B ->137B	-0.32915

Excited State 16: 3.047-A 3.8100 eV 325.42 nm f=0.0003 <S**2>=2.072

129A ->137A	0.11549
130A ->139A	0.20263
130A ->140A	0.15012
131A ->139A	0.11427
131A ->140A	-0.15015
132A ->137A	0.11632
135A ->138A	-0.30167
136A ->138A	-0.16241
136A ->141A	0.41006
136A ->142A	0.10585
136A ->143A	-0.16058
128B ->136B	-0.15329
129B ->137B	-0.10904
130B ->139B	-0.20265
130B ->140B	-0.14348
131B ->139B	-0.10794
131B ->140B	0.15328
135B ->138B	0.52873

Excited State 17: 2.946-A 3.8375 eV 323.09 nm f=0.0074 <S**2>=1.920

130A ->139A	-0.23047
130A ->140A	-0.16444
131A ->139A	-0.16207
131A ->140A	0.21096
132A ->139A	-0.10399
135A ->138A	-0.20607
136A ->138A	-0.12945
136A ->141A	0.20783
136A ->142A	0.16198
128B ->136B	0.51915
129B ->137B	0.13073
130B ->139B	0.20687
130B ->140B	0.14148
131B ->139B	0.13237

131B ->140B	-0.19037
132B ->137B	0.11099
132B ->139B	0.10418
135B ->138B	0.37038

Excited State 18: 2.157-A 3.8467 eV 322.31 nm f=0.0059 <S**2>=0.913
 136A ->142A 0.95237
 135B ->138B -0.12607

Excited State 19: 2.749-A 3.9669 eV 312.55 nm f=0.0132 <S**2>=1.640
 133A ->138A 0.11395
 134A ->138A -0.17903
 135A ->144A -0.16330
 136A ->143A -0.14024
 136A ->144A 0.75931
 129B ->136B -0.12374
 129B ->138B -0.10879
 133B ->138B -0.12493
 134B ->138B -0.38945
 135B ->143B 0.18108
 135B ->144B 0.12614

Excited State 20: 2.286-A 4.0051 eV 309.56 nm f=0.0191 <S**2>=1.056
 135A ->141A -0.10015
 136A ->143A 0.89751
 136A ->144A 0.11885
 136A ->145A -0.11633
 128B ->136B 0.12757
 135B ->138B 0.14422

CzBTM (UB3LYP/6-31G(d))

Excited State 1: 2.054-A 2.1841 eV 567.66 nm f=0.0884 <S**2>=0.805
 134B ->136B 0.98732

This state for optimization and/or second-order correction.

Total Energy, E(TD-HF/TD-KS) = -3775.72796568

Copying the excited state density for this state as the 1-particle RhoCI density.

Excited State 2: 2.071-A 2.2525 eV 550.44 nm f=0.0000 <S**2>=0.822
 135B ->136B 0.98789

Excited State 3: 2.189-A 2.5933 eV 478.10 nm f=0.0459 <S**2>=0.948
 134A ->137A 0.14669

136A ->137A	0.89734
130B ->136B	0.26852
133B ->136B	-0.16207

Excited State 4:	2.101-A	2.9832 eV	415.61 nm	f=0.0015	<S**2>=0.854
134A ->138A	0.11167				
136A ->138A	0.92344				
132B ->136B	-0.32141				

Excited State 5:	2.143-A	3.0405 eV	407.78 nm	f=0.0000	<S**2>=0.898
136A ->139A	0.91110				
131B ->136B	-0.34298				

Excited State 6:	2.647-A	3.1103 eV	398.62 nm	f=0.0219	<S**2>=1.501
134A ->144A	0.14277				
135A ->139A	-0.17378				
135A ->140A	0.26257				
136A ->137A	0.19986				
136A ->144A	-0.17897				
133B ->136B	0.74607				
134B ->144B	-0.15845				
135B ->136B	-0.11875				
135B ->139B	0.24022				
135B ->140B	-0.26009				

Excited State 7:	2.456-A	3.2077 eV	386.53 nm	f=0.0174	<S**2>=1.258
130A ->137A	-0.21617				
131A ->139A	0.12243				
132A ->138A	0.13538				
133A ->137A	0.10581				
134A ->141A	0.13970				
136A ->139A	0.11707				
136A ->141A	0.46339				
136A ->143A	-0.22438				
129B ->136B	0.58891				
130B ->137B	0.18681				
131B ->136B	0.33716				
131B ->139B	-0.11120				
132B ->138B	-0.14590				

Excited State 8:	2.364-A	3.2322 eV	383.59 nm	f=0.0027	<S**2>=1.147
134A ->139A	0.12685				
136A ->139A	-0.23116				
136A ->140A	0.79280				

129B ->136B	0.15053
131B ->136B	-0.42694
134B ->139B	-0.14819
134B ->140B	0.13510

Excited State 9: 2.816-A 3.2399 eV 382.67 nm f=0.0716 <S**2>=1.733

134A ->137A	0.12109
134A ->144A	0.10699
135A ->139A	-0.23072
135A ->140A	0.34293
136A ->137A	-0.28865
136A ->138A	-0.15064
136A ->144A	-0.12932
130B ->136B	0.44110
132B ->136B	-0.31511
133B ->136B	-0.32940
134B ->144B	-0.12483
135B ->139B	0.27565
135B ->140B	-0.29377

Excited State 10: 2.211-A 3.3156 eV 373.95 nm f=0.0129 <S**2>=0.973

135A ->139A	-0.10505
135A ->140A	0.15097
136A ->138A	0.30309
130B ->136B	0.18454
132B ->136B	0.85729
133B ->136B	-0.21690
135B ->140B	-0.10231

Excited State 11: 2.190-A 3.3541 eV 369.65 nm f=0.0040 <S**2>=0.949

136A ->139A	0.25329
136A ->140A	0.49768
136A ->141A	-0.21467
129B ->136B	-0.18267
131B ->136B	0.73733
134B ->139B	-0.10590

Excited State 12: 2.466-A 3.3724 eV 367.64 nm f=0.0601 <S**2>=1.270

134A ->137A	0.14768
135A ->139A	0.19156
135A ->140A	-0.27042
136A ->137A	-0.19760
130B ->136B	0.70578
133B ->136B	0.45666

135B ->139B -0.16160
135B ->140B 0.16693

Excited State 13: 2.427-A 3.6766 eV 337.23 nm f=0.0692 <S**2>=1.222
130A ->137A 0.12752
132A ->138A -0.10981
133A ->144A -0.10316
136A ->140A 0.11110
136A ->141A 0.79650
136A ->143A 0.16766
136A ->145A 0.13152
129B ->136B -0.32267
131B ->139B 0.10274
132B ->138B 0.12430

Excited State 14: 3.132-A 3.7491 eV 330.71 nm f=0.0163 <S**2>=2.202
131A ->138A -0.29335
132A ->139A -0.23860
132A ->140A -0.12681
134A ->137A -0.35155
136A ->137A 0.11616
136A ->142A -0.31157
129B ->137B -0.14822
130B ->136B 0.37062
131B ->138B 0.27276
132B ->139B 0.20430
132B ->140B 0.15272
133B ->136B -0.11239
134B ->137B 0.42153

Excited State 15: 2.252-A 3.7625 eV 329.52 nm f=0.0018 <S**2>=1.018
134A ->137A -0.16884
136A ->142A 0.92959
134B ->137B 0.13475

Excited State 16: 3.044-A 3.8397 eV 322.90 nm f=0.0131 <S**2>=2.066
130A ->137A 0.17200
130A ->138A -0.13171
131A ->139A -0.31759
131A ->140A -0.16533
132A ->138A -0.35148
136A ->145A -0.10333
129B ->136B 0.54649
130B ->137B -0.20330

131B ->139B	0.25842
131B ->140B	0.18987
132B ->138B	0.32369
133B ->137B	0.11045
134B ->139B	-0.11554

Excited State 17: 2.666-A 3.9067 eV 317.36 nm f=0.0105 <S**2>=1.527

129A ->140A	-0.10552
133A ->144A	0.15633
134A ->139A	0.13370
134A ->140A	-0.15597
134A ->141A	0.13439
136A ->140A	-0.15509
136A ->141A	0.14815
136A ->143A	0.70734
136A ->145A	-0.11518
128B ->136B	-0.14821
132B ->138B	-0.10784
133B ->144B	-0.14286
134B ->139B	-0.29648
134B ->140B	0.22305
134B ->141B	-0.12021
135B ->146B	0.10144

Excited State 18: 2.364-A 3.9699 eV 312.31 nm f=0.0229 <S**2>=1.147

134A ->140A	0.10508
136A ->141A	-0.12410
136A ->143A	0.50171
128B ->136B	0.63496
129B ->136B	0.26711
134B ->139B	0.30262
134B ->140B	-0.22844

Excited State 19: 2.750-A 3.9980 eV 310.11 nm f=0.0066 <S**2>=1.641

134A ->144A	-0.18977
136A ->144A	0.78281
133B ->136B	0.12091
133B ->139B	0.11049
133B ->140B	-0.11690
134B ->144B	0.26613
135B ->139B	0.30040
135B ->140B	-0.24942

Excited State 20: 2.867-A 4.0049 eV 309.58 nm f=0.0003 <S**2>=1.805

134A ->139A	0.10012
134A ->140A	-0.12709
135A ->137A	0.85655
135A ->144A	-0.11008
136A ->140A	-0.11693
136A ->143A	-0.17630
128B ->136B	0.28837
134B ->139B	-0.20484
134B ->140B	0.15518